

# Analytical study on the criticality of the Stochastic Optimal Velocity model

Masahiro Kanai<sup>1</sup>, Katsuhiro Nishinari<sup>2</sup>, Tetsuji Tokihiro<sup>1</sup>

<sup>1</sup> Graduate School of Mathematical Sciences, University of Tokyo, 3-8-1 Komaba, Tokyo 153-8914, Japan

<sup>2</sup> Department of Aeronautics and Astronautics, Faculty of Engineering, University of Tokyo, 7-3-1 Hongo, Tokyo 113-8656, Japan

E-mail: kanai@ms.u-tokyo.ac.jp

**Abstract.** In recent works, we have proposed a stochastic cellular automaton model of traffic flow connecting two exactly solvable stochastic processes, i.e., the Asymmetric Simple Exclusion Process and the Zero Range Process, with an additional parameter. It is also regarded as an extended version of the Optimal Velocity model, and moreover it shows particularly notable properties. In this paper, we report that when taking Optimal Velocity function to be a step function, all of the flux-density graph (i.e. the fundamental diagram) can be estimated. We first find that the fundamental diagram consists of two line segments resembling an *inversed*- $\lambda$  form, and next identify their end-points from a microscopic behaviour of vehicles. It is notable that by using a microscopic parameter which indicates a driver's sensitivity to the traffic situation, we give an explicit formula for the critical point at which a traffic jam phase arises. We also compare these analytical results with those of the Optimal Velocity model, and point out the crucial differences between them.

PACS numbers: 05.60.-k, 05.45.-a, 05.70.Jk, 45.70.Vn, 89.40.-a

Submitted to: *J. Phys. A: Math. Gen.*

## 1. Introduction

Traffic dynamics has naturally attracted much attention from engineers since the volume of vehicular traffic outstripped road capacity [1, 2, 3]. Especially for the last decades, it has attracted a lot of interest, in addition, from physicists and mathematicians as a typical example of non-equilibrium statistical mechanics of self-driven many particle systems [1]. Since self-driven particles do not obey Newton's laws of motion, their collective phenomena are far from predictable and are strongly dependent on their density. Recently, a number of different approaches to the subject have been made from various viewpoints such as microscopic and macroscopic, continuous and discrete, deterministic and stochastic.

The Burgers equation  $\rho_t = 2\rho\rho_x + \rho_{xx}$ , is known as an elementary model of traffic flow. It formulates the evolution of density distribution of vehicles, i.e., it is a macroscopic, continuous model. Recent studies show that the Burgers equation is directly connected with other basic models of traffic flow [4]. The Burgers equation is, at first, transformed into a cellular automaton (CA) model (a microscopic discrete one) through *ultra-discretization* [5]. Note that CA models are microscopic ones because they explicitly define each particle's motion. It provides a method to reveal another profile of models, and enables us to return from macroscopic to microscopic. From the Burgers equation, we thereby obtain the so-called *Burgers cellular automata* (BCA), which is an extension of the Rule-184 CA [4]. This CA has a very simple update rule, i.e., if the adjacent site is not occupied, the vehicle move ahead with a given probability, but otherwise it does not. Each site contains one vehicle at most, and the rule is generally called *the hard-core exclusion rule*. In the case of BCA, each site can contain more than one vehicle.

Moreover, BCA can be transformed into another basic model, i.e., the *Optimal Velocity (OV) model*, through the *discrete Euler-Lagrange (E-L) transformation*. The discrete E-L transformation is made on fully discrete variables, and then field variables change to particle variables [4]. The OV model is a continuous, microscopic model, and is expressed as

$$\ddot{x}_i = a[V(x_{i+1} - x_i) - \dot{x}_i], \quad (1)$$

where  $x_i = x_i(t)$  denotes the position of the  $i$ -th vehicle at time  $t$  and the function  $V$  is called the *Optimal Velocity (OV) function* [6, 7]. The OV function gives the optimal velocity of a vehicle in terms of the headway  $x_{i+1} - x_i$ , where the  $i$ -th vehicle follows the  $(i + 1)$ -th in the same lane, and then the OV function, in general, is monotonically increasing. In particular, the OV model obtained from BCA has OV function which is a step function. This suggests that the OV model with a step function is essential as well as elementary.

Cellular automaton models are efficient and flexible compared to those described by differential equations, and they have been used to model complex traffic systems such as ramps and crossings [2]. The Nagel-Schreckenberg (N-S) model, a well-known CA model, successfully reproduces typical properties of real traffic [8]. What makes it

sophisticated is a *random braking rule*, which is a plausible mechanism to simulate the motion of vehicles in a single lane. Nevertheless, the N-S model does not succeed in reproducing the so-called *metastable state*, i.e., an unstable state which breaks down to the lower-flux stable state under some perturbations.

Extensive study of traffic flow has revealed that the metastable property, appearing in the medium density region, is universal in real traffic flows, and accordingly that property is essential in modelling [9, 10]. Moreover, it is quite distinct among non-equilibrium statistical systems [1]. In other words, this metastable property plays a critical role in characterizing traffic flow from the viewpoint of dynamics, and it is hence required for traffic models to exhibit this property. Thus far, one needs the *slow-start rule* to reproduce a metastable state in existing CA models [10, 11, 12, 13]. It introduces a delay for vehicles to respond to the changing traffic situation, i.e., if a vehicle stops due to the hard-core exclusion rule, the slow-start rule forces it to stop again at the next time step. In contrast, due to the second-order derivative, the OV model naturally includes a similar mechanism to the slow-start rule. The intrinsic parameter  $a$  in the OV model (1) corresponds to the driver's sensitivity to a traffic situation (e.g. the distances relatively to the vehicles ahead), and plays an important role in the stability of a traffic flow. Note that the reciprocal of  $a$  represents a driver's response time, connecting the OV model and the Newell model [14].

In the next section, we introduce a stochastic CA model following [15], and then we show that the model inherits the sophisticated features from the OV model.

## 2. Stochastic optimal velocity model

Most stochastic models incorporate noise, taking into account uncertain effects such as different driver characteristics, driver error false operation, and external influences. In general, randomness disturbs metastable states and thus stochastic models do not show any metastable state in the fundamental diagram. In contrast, as will be seen in the latter part of this paper, the probability of the SOV model plays an essential role in producing metastable states, and the metastable states emerge by extracting a deterministic mechanism. Note that a similar trick was considered in [21].

### 2.1. General scheme

First of all, we explain the general framework of our stochastic CA model for one-lane traffic. The roadway, being divided into cells, is regarded as a one-dimensional array of  $L$  sites, and each site contains one vehicle at most. Let  $\mathbf{M}_i^t$  be a stochastic variable which denotes the number of sites through which the  $i$ -th vehicle moves at time  $t$ , and  $w_i^t(m)$  be the probability that  $\mathbf{M}_i^t = m$  ( $m = 0, 1, 2, \dots$ ). Then, we assume a principle of motion that the probability  $w_i^{t+1}(m)$  depends on the probability distribution  $w_i^t(0), w_i^t(1), \dots$ , and the positions of vehicles  $x_1^t, x_2^t, \dots, x_N^t$  at the previous time. The updating procedure is as follows:

- Calculate the next intention  $w_i^{t+1}$  ( $i = 1, 2, \dots, N$ ) from the present, intention  $w_i^t(0), w_i^t(1), \dots$  and positions  $x_1^t, x_2^t, \dots, x_N^t$ ;

$$w_i^{t+1}(m) = f(w_i^t(0), w_i^t(1), \dots; x_1^t, \dots, x_N^t; m) \quad (2)$$

- Determine the number of sites  $M_i^{t+1}$  through which a vehicle moves (i.e. the velocity) probabilistically according to the intention  $w_i^{t+1}$ .
- The new position of each vehicle is

$$x_i^{t+1} = x_i^t + \min(\Delta x_i^t, M_i^{t+1}) \quad (\forall i), \quad (3)$$

where  $\Delta x_i^t = x_{i+1}^t - x_i^t - 1$  denotes the headway. (Headway is defined to be the clear space in front of the vehicle, and thus in a CA model we need to subtract 1 to take account of the site occupied by the vehicle itself.)

The hard-core exclusion rule is incorporated through the second term of the right hand side of (3).

We call the probability distribution  $w_i^t$  *the intention* because it is an intrinsic variable of the vehicle and drives themselves. It brings uncertainty of operation into the traffic model and has no physical counterpart.

## 2.2. The SOV model

In what follows, we assume  $w_i^t(m) \equiv 0$  for  $m \geq 2$ . It is notable that  $\sum_{m=0}^{\infty} w_i^t(m) = 1$  by definition and the expectation value  $\langle M_i^t \rangle = \sum_{m=0}^{\infty} m w_i^t(m)$ , and hence, setting  $v_i^t = w_i^t(1)$ , we have  $w_i^t(0) = 1 - v_i^t$  and  $\langle M_i^t \rangle = v_i^t$ . From (2) we have

$$\begin{cases} w_i^{t+1}(1) = v_i^{t+1} = f(v_i^t; x_1^t, x_2^t, \dots; 1) \\ w_i^{t+1}(0) = 1 - v_i^{t+1}, \end{cases} \quad (4)$$

and we therefore express the intention by  $v_i^t$  in stead of  $w_i^t$ . As long as vehicles move separately (i.e.  $\Delta x_i^t \gg 0$ ), the positions are updated according to the simple form

$$x_i^{t+1} = \begin{cases} x_i^t + 1 & \text{with probability } v_i^{t+1} \\ x_i^t & \text{with probability } 1 - v_i^{t+1}, \end{cases} \quad (5)$$

and consequently we have

$$\langle x_i^{t+1} \rangle = \langle x_i^t \rangle + v_i^{t+1} \quad (6)$$

in the sense of expectation value. This equation expresses the fact that the intention  $v_i^{t+1}$  can be regarded as the average velocity at time  $t$ .

Let us take an evolution equation

$$v_i^{t+1} = (1 - a)v_i^t + aV(\Delta x_i^t), \quad (7)$$

in (2), where  $a$  ( $0 \leq a \leq 1$ ) is a parameter and the function  $V$  takes the value in  $[0, 1]$  so that  $v_i^t$  should be within  $[0, 1]$ . Equation (7) consists of two terms, i.e., a term turning over the intention  $v_i^t$  into the next, and an effect of the situation (the headway  $\Delta x_i^t$ ). The intrinsic parameter  $a$  indicates the sensitivity of vehicles to the traffic situation, and the larger  $a$  is, the less time a vehicle takes to change its intention.

A discrete version of the OV model is expressed as

$$x_i(t + \Delta t) - x_i(t) = v_i(t)\Delta t, \quad (8)$$

$$v_i(t + \Delta t) - v_i(t) = a[V(\Delta x_i(t)) - v_i(t)]\Delta t, \quad (9)$$

where  $\Delta x_i(t) = x_{i+1}(t) - x_i(t)$ , and  $\Delta t$  is a time interval. Due to the formal correspondence between (7) and (9), we call a stochastic CA model defined by (7) the *Stochastic Optimal Velocity (SOV) model*, hereafter.

As we noted in the preceding work [15], the SOV model reduces to two exactly solvable stochastic models, the Asymmetric Simple Exclusion Process (ASEP) [16, 17] and the Zero Range Process (ZRP) [18, 19], when the parameter  $a$  ( $0 \leq a \leq 1$ ) takes the values of 0 and 1 respectively. The SOV model has a fundamental diagram similar to that of ZRP as  $a$  approaches 1 (the ZRP limit). However, when  $a$  takes a small value (the ASEP limit), the SOV model shows quite different properties from those of ASEP. Since we already discussed this point in detail [15], we do not devote any space to the limiting case  $a \rightarrow 0$ . It should be noted here that a model including ZRP and ASEP was proposed in [20]. However, this model does not satisfy the essential standard that a traffic model should reproduce the metastable state observed universally in empirical traffic data.

### 3. The SOV model with a step OV function

In this section, we take a step function

$$V(x) = \begin{cases} 0 & (0 \leq x < d) \\ 1 & (x \geq d) \end{cases} \quad (10)$$

as the OV function. Then, we impose a periodic boundary condition and adopt the parallel updating as usual.

#### 3.1. Comparison with the OV model

In preceding works [22, 23], the original OV model with the step OV function (10) has been studied in detail. In an ideal case, they gave an exact solution for cluster formation (i.e. the traveling cluster solution). They use figures to illustrate the behaviour of vehicles forming a cluster, and find a closed loop or *hysteresis loop* in the velocity-headway diagram (phase space). Moreover, from the microscopic viewpoint, they evaluate the velocity of a jam transmitting backward, and two specific headways; the distance  $\Delta x_J$  with which vehicles stop in a jam, and  $\Delta x_F$  with which vehicles move in a free-flow region. (See §3.4.)

Figure 1 shows the phase space of our model. Note that the vertical axis of Figure 1 means the expectation value of velocity. We find that there appears a hysteresis loop corresponding to Figure 3 in [22]. Since our model incorporates the hard-core exclusion rule as well as a CA model with maximum allowed velocity 1, it takes a different shape from the parallelogram of Figure 3 in [22]. Note that, in contrast with the original OV

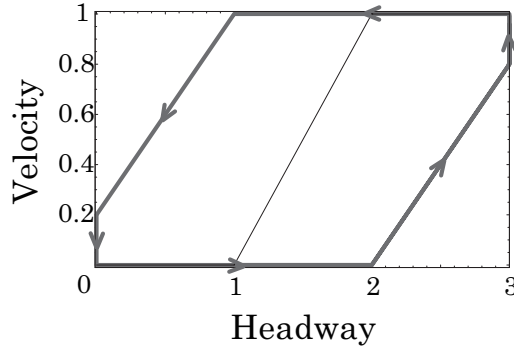


**Figure 1.** The headway-velocity diagram (phase space) of the SOV model ( $a = 0.8$ ) with a step function ( $d = 2$ ). We observe a hysteresis loop (thick gray line) around the discontinuous point of the step OV function (thin black line), where the phase of a vehicle goes round in the direction of arrows. In comparison with Fig. 3 of [22], two corners of the parallelogram are folded by an effect of the hard-core exclusion rule.

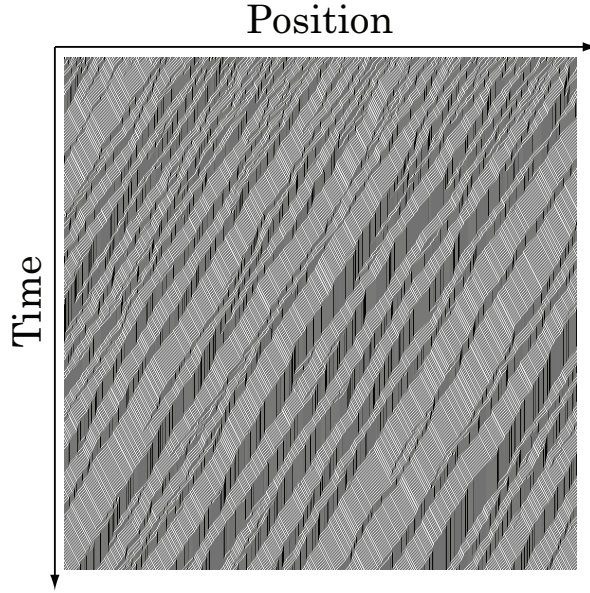


**Figure 2.** The spatio-temporal pattern of the SOV model ( $a = 0.8$ ) with a step function ( $d = 2$ ) simulated with the number of site  $L = 1000$  and the number of vehicles  $M = 400$ , where periodic boundary condition is imposed on the roadway. There appear a lot of stable clusters (small jams) propagating backward.

model, our model contains the element of randomness and hence the vehicles do not always move in accordance with the hysteresis loop. In Figure 2, we show the spatio-temporal pattern of our model, which should be compared with Figure 4 in [22]. Due to the randomness, the clusters do not hold their sizes constant and the number of them fluctuates with time.

These two figures suggest that the SOV model inherits, from the original OV model, the mechanism of vehicles clustering and then separating. However, from the

viewpoint of many-particle systems, the SOV model shows apparently different collective phenomena from that of the OV model. In the following part of this section, we estimate the fundamental diagram of the SOV model with a step function as well as comparing the estimated specific headways and velocity of our model with those given in [22].

### 3.2. Fundamental diagram

We denote the density of vehicles to sites by  $\rho = N/L$  ( $L$  is the number of sites, and  $N$  the number of vehicles), which is a macroscopic variable, and a conserved quantity of motion under the periodic boundary condition, no entrances or exits. Another macroscopic variable flux,  $Q = \rho v$ , is defined using the average velocity in a steady state;

$$v := \frac{1}{N} \sum_{i=1}^N (x_i^T - x_i^{T-1}), \quad (11)$$

where time  $T$  should be taken large enough for the system to reach a steady state.

A *fundamental diagram*, a plot of the flux versus the density, illustrates how traffic conditions depend on density. It represents the characteristics of a traffic model, and hence traffic models are required to reproduce a fundamental diagram observed in real traffic flow. As far as the above-mentioned exactly solvable models (ASEP and ZRP) are concerned, we can make an exact calculation of the fundamental diagram [25, 26]. We only exhibit an explicit formula of the fundamental diagram of ZRP (i.e.  $a = 1$ ) especially when a step function is adopted as the OV function:

$$Q^{\text{ZRP}}(\rho) = \begin{cases} \min(\rho, 1 - d\rho) & (0 \leq \rho \leq \frac{1}{d}) \\ 0 & (\frac{1}{d} < \rho \leq 1) \end{cases} \quad (12)$$

where  $d$  is the discontinuous point of the step OV function (10).

Since the flux of R184-CA (ASEP with the hopping probability  $p = 1$ ) is obtained in the simple form of  $Q(\rho) = \min(\rho, 1 - \rho)$ , considering that each vehicle occupies  $d$  sites, we directly obtain the formula (12).

### 3.3. Metastable state

Figure 3 shows the fundamental diagram of the SOV model with the step OV function (10). We find that the diagram consists of two lines corresponding respectively to *free-flow* phase (positive slope) and *jam* phase (negative slope). It is remarkable that there is a region of density where two states (a free-flow state and a jam state) coexist. The second-order difference allows the model to show this property, so-called *hysteresis*, as pointed out in Section 1.

The free-flow line in the fundamental diagram has a slope of 1, i.e., all the vehicles are moving deterministically (i.e.  $v_i^t = 1$ ) without jamming. This kind of state can be implemented in the uniform state; equal spacing of vehicles and the initial velocity  $v_i^0 = 1$  for all  $i$ . As can be seen from (7), the intention changes

$$\begin{cases} v_i^t = 1 - (1 - v_i^0)(1 - a)^t & (\Delta x_i^t \geq d), \\ v_i^t = v_i^0(1 - a)^t & (\Delta x_i^t < d), \end{cases} \quad (13)$$

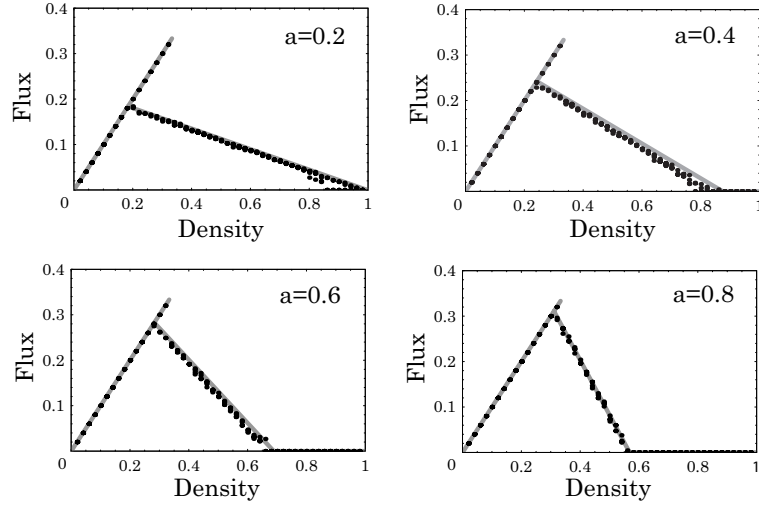


**Figure 3.** The fundamental diagram of the SOV model with the step OV function (10) plotted at each value of sensitivity parameter  $a$ , where the discontinuous point is  $d = 2$ , the initial value of the intention is  $v_i^0 = 1$ , and the system size is  $L = 1000$ . Theoretical curve (gray) has a complete agreement with simulated data (dots) in these cases.

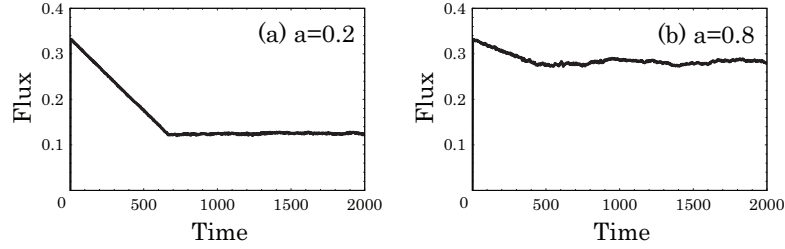


**Figure 4.** The flux decreases rapidly as an external perturbation is imposed, and finally settles into a lower value, i.e., the flux of jam state. We simulate with the number of sites  $L = 1000$ , the number of vehicles  $M = 334$ , and the sensitivity parameter takes the value of (a)  $a = 0.2$  and (b)  $a = 0.8$ . It implies that, in contrast with our preceding paper, the metastable state has no lifetime.

and consequently the uniform states constitute a line segment

$$Q = \rho \quad (0 \leq \rho \leq \rho_h) \quad (14)$$

in the fundamental diagram. The maximum-flux density  $\rho_h$ , at which the vehicles take the minimum value  $d$  of equal spacing, is given as follows:

$$\rho_h = \frac{1}{1+d}. \quad (15)$$

In Figure 3, we see that the formula (15) is in the complete agreement with the simulated results in the case of  $d = 2$ .

The uniform states divide into two classes especially under an external perturbation which makes a vehicle accidentally slow down. One is a class of the states recovering their uniform configurations, and the other is that of the states never recovering them.



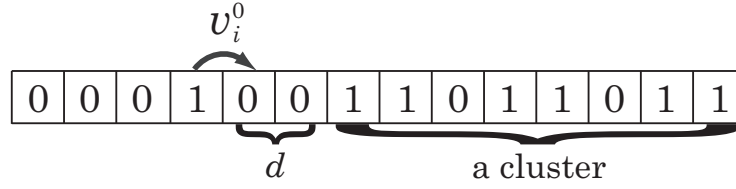


**Figure 5.** Schematic picture of the case that a free vehicle reduces its intention  $v_i^0 = 1$  approaching a cluster, and finally comes to be in the cluster. The vehicle stops with a headway to the cluster ahead, which is estimated from the OV function.

In this paper, we call such a state unstable against external perturbations a *metastable state* in accordance with customary practice. Figure 4 shows that, under perturbation, the flux of a metastable state is decreasing and tends to that of a jam state. (Note that it also implies that there is not such a long-lived metastable state as observed in [15].) Consequently, in the region of density where two states coexist, the uniform states appear as a metastable, higher-flux branch.

#### 3.4. The critical point of phase transition

The flux of traffic flow increases in proportion to the density of vehicles while the density is small. However, as the density becomes bigger, close-range interaction between vehicles makes a wide, strong correlation over them, and consequently gives rise to a jam. Then, there appears a turning point at which the flux declines for the first time. Around that point (the so-called *critical point*), the states of traffic flow bifurcates into a stable branch and a metastable branch, and moreover phase transition occurs between them.

In order to estimate the critical point, we consider that the jam line should be expressed by

$$Q = \frac{\rho_c}{\rho_{\max} - \rho_c}(\rho_{\max} - \rho), \quad (16)$$

where  $\rho_{\max}$  and  $\rho_c$  denote respectively the density at which flux vanishes and that of the critical point. From (16) and  $Q = \rho v$ , we have

$$\frac{1 - \rho}{\rho} = \frac{1 - \rho_{\max}}{\rho_{\max}}(1 - v) + \frac{1 - \rho_c}{\rho_c}v. \quad (17)$$

Equation (17) suggests that the spatial pattern divides into two kinds, i.e., clustering ( $v = 0$ ) and free flow ( $v = 1$ ). Then, since the vehicles move at velocity 1 or 0 in the present model,  $v$  just indicates the ratio of those in free flow, and moreover total average headway  $\langle \Delta x \rangle = (1 - \rho)/\rho$  is calculated from the average headway of the clustered vehicles  $\langle \Delta x_J \rangle = (1 - \rho_{\max})/\rho_{\max}$  and that of the vehicles in free flow  $\langle \Delta x_F \rangle = (1 - \rho_c)/\rho_c$ . These two values reflect a macroscopic property of the SOV model with the OV function (10), but we should estimate them from a microscopic viewpoint. In what follows, we consider the case of  $d = 2$ , following [22].

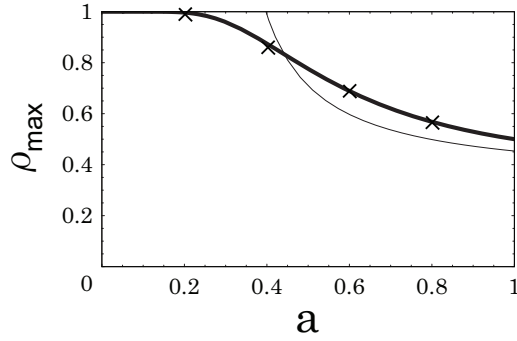


**Figure 6.** The theoretical curve of the maximum density  $\rho_{\max}$  (thick line) at which the flux vanishes with the corresponding numerical results (cross). They have perfect agreement. We also show a corresponding curve of the original OV model (thin line) by use of (21).

First, we think of  $\rho_{\max}$  as the limit density at which all free-flow domains of the roadway close up and no vehicle can move then. Let us consider the situation illustrated in Figure 5 that a free vehicle with its intention 1 is going into a cluster. Then, taking the time  $t = 0$  when the headway firstly gets equal to  $d$ , the intention decreases as  $v_i^t = (1 - a)^t$ . Since it gives the probability of the vehicle moving at  $t$ , the average headway, while in cluster, amounts to

$$\langle \Delta x_J \rangle = \prod_{t=1}^{\infty} (1 - v_i^t) \quad (18)$$

$$= \left[ \frac{\vartheta_4(0, 1-a)^4 \vartheta_2(0, 1-a) \vartheta_3(0, 1-a)}{2(1-a)^{1/4}} \right]^{1/6}, \quad (19)$$

where  $\vartheta_k(u, q)$  ( $k = 1, 2, 3, 4$ ) are the elliptic theta functions. Consequently, we obtain the density of clustering vehicles

$$\rho_{\max} = \frac{1}{1 + \langle \Delta x_J \rangle}, \quad (20)$$

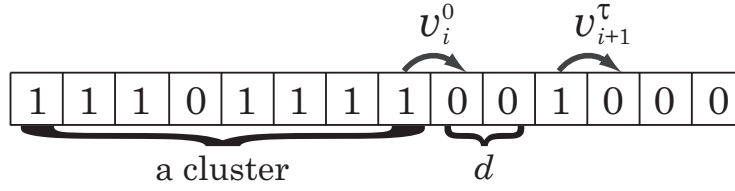
as a function of the sensitivity parameter  $a$ . Note that  $0 \leq \langle \Delta x_J \rangle \leq 1$  since  $d = 2$ , and  $\langle \Delta x_J \rangle$  is equivalent to the probability of  $\Delta x_i^t$  taking the value of 1.

Figure 6 shows the graph of  $\rho_{\max}$ , and it has a perfect agreement with the numerical results read off from Figure 3. In [22], they give the explicit formula of  $\Delta x_J$ , the uniform headway with which vehicles stop in a jam. It reads

$$\Delta x_J = d - \frac{v_{\max} \sigma}{2a}, \quad (21)$$

where  $d = 2$  and  $v_{\max} = 1$  in the present case, and  $\sigma \simeq 1.59$ . By use of (21), we illustrate the corresponding graph in Fig. 6 as well. Since the original OV model does not incorporate a hard-core exclusion rule, the sensitivity parameter  $a$  is limited in the scope of  $\Delta x_J \geq 0$  so as to avoid any collision. In contrast, the maximum density of the SOV model is retained, due to that rule, not to diverge within  $0 \leq a \leq 1$ .

Next, in order to estimate  $\langle \Delta x_F \rangle$  we consider that two vehicles in the front of a cluster are getting out of it as illustrated in Figure 7. Then, as described above,



**Figure 7.** Schematic picture of the situation that two adjacent vehicles in the front of a cluster recover their intention and get out of the cluster. We estimate the headway with which the two vehicles finally come to move free.

there occur two cases since  $d = 2$ ;  $\Delta x_i^0 = 1$  with probability  $\langle \Delta x_J \rangle$  and  $\Delta x_i^0 = 0$  with probability  $1 - \langle \Delta x_J \rangle$ , where we again take the time  $t = 0$  when  $\Delta x_i^t$  becomes  $d$ . Corresponding to  $\Delta x_i^0 = 0$  and  $1$ , we describe  $\langle \Delta x_F \rangle$  respectively as  $\langle \Delta x_F \rangle_0$  and  $\langle \Delta x_F \rangle_1$ , and accordingly our main result is expressed as follows:

$$\rho_c = \frac{1}{1 + \langle \Delta x_F \rangle}, \quad (22)$$

where

$$\langle \Delta x_F \rangle = \langle \Delta x_F \rangle_1 \langle \Delta x_J \rangle + \langle \Delta x_F \rangle_0 (1 - \langle \Delta x_J \rangle). \quad (23)$$

Let  $\tau$  denote the interval of time for the front vehicle to get out of the cluster. Provided that clusters are large enough to take approximately  $v_i^0 = 0$  and that the second vehicle leaving the cluster maintains a headway of at least  $d$ , we conclude that  $v_i^0 = 0$ ,  $v_{i+1}^0(\tau) = 1 - (1 - a)^\tau$ ,  $v_i^t = 1 - (1 - a)^t$ , and  $v_{i+1}^t(\tau) = 1 - (1 - a)^{\tau+t}$  from (13). Note that  $\tau$  is a stochastic valuable, and hence  $v_{i+1}^0$  and  $v_{i+1}^t$  are dependent on  $\tau$ .

In the case of  $\Delta x_i^0 = 1$ : Since  $v_i^t$  indicates the probability of moving ahead at one site, the probability of  $\tau = t$  amounts to

$$P_1(\tau = t) = v_i^t \prod_{s=1}^{t-1} (1 - v_i^s) \quad (24)$$

and moreover, the distance which the two make in free flow amounts to

$$\sum_{t=1}^{\infty} [v_{i+1}^t(\tau) - v_i^t] = \frac{1-a}{a} v_{i+1}^0(\tau). \quad (25)$$

Consequently, we have  $\langle \Delta x_F \rangle_1$  in a convenient form for computation:

$$\langle \Delta x_F \rangle_1 = d + \sum_{\tau=1}^{\infty} \frac{1-a}{a} v_{i+1}^0(\tau) P_1(\tau) \quad (26)$$

$$= 1 + \frac{\vartheta_2(0, \sqrt{1-a})}{2(1-a)^{1/8}}. \quad (27)$$

In the case of  $\Delta x_i^0 = 0$ : The probability of  $\tau = t$  amounts to

$$P_0(\tau = t) = v_i^t \sum_{s=1}^{t-1} \left[ v_i^s \prod_{r=1, r \neq s}^{t-1} (1 - v_i^r) \right] \quad (28)$$

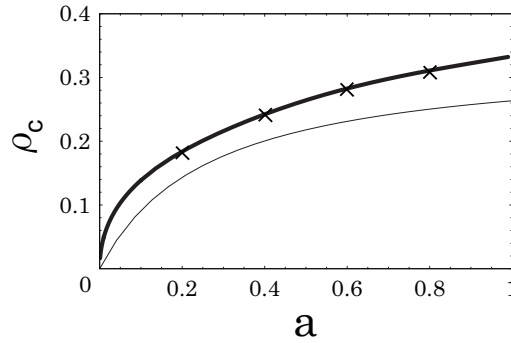


**Figure 8.** The theoretical curve of the critical density  $\rho_c$  (thick line) at which the flux bifurcates into a metastable branch and a stable jam branch (i.e. hysteresis), with the corresponding numerical results (cross). They also have a perfect agreement. The corresponding curve (thin line) of the original OV model is illustrated by use of (30).

Consequently, from (13) we have

$$\langle \Delta x_F \rangle_0 = d + \sum_{\tau=1}^{\infty} \left[ \frac{1-a}{a} v_{i+1}^0(\tau) P_0(\tau) \right], \quad (29)$$

and finally  $\langle \Delta x_F \rangle$  is formulated as a function of the sensitivity parameter  $a$ .

The formula of  $\Delta x_F$  in the corresponding case of the OV model, given in [22], reads

$$\Delta x_F = d + \frac{v_{\max} \sigma}{2a}, \quad (30)$$

where  $d = 2$ ,  $v_{\max} = 1$ , and  $\sigma = 1.59$ . Figure 8 shows the critical density  $\rho_c$  versus the sensitivity parameter  $a$ . It also has a perfect agreement with the numerical results read out from Fig. 3. By use of (30), we illustrate the corresponding graph in Fig. 8 as well. We find that the two theoretical curves present a qualitative agreement, while there are some quantitative differences due to the choice of unit car size.

#### 4. Summary and Conclusion

The Stochastic Optimal Velocity model was introduced in the preceding paper [15] as a stochastic cellular automaton model extending two exactly solvable models (the Asymmetric Simple Exclusion Process and the Zero Range Process). Moreover, since it has the same formulation as the Optimal Velocity model, the SOV model can be regarded as a stochastic extension of the OV model.

In the present paper, we take a step function as the OV function in order to investigate an elementary property of the SOV model. In previous papers [22, 23], the original OV model with this OV function are studied in detail and some analytical results are given. Accordingly, we first make a qualitative comparison between them in terms of the motion of each vehicle, and then we see a similar hysteresis loop in the velocity-headway diagram (phase space) as long as the density is low. That is, as far as each vehicle's motion is concerned, the vehicles of the two models show a similar motion within a low-density region.

However, as the density of vehicles grows large, the structural difference between ordinary differential equations and cellular automata, as well as the presence or absence of randomness, causes crucial differences especially in the fundamental diagram. As discussed in [6], the metastability observed in the OV model is derived from the instability of a uniform/homogeneous flow against perturbations. In general, randomness introduced in traffic models tends to eliminate metastable states as well as unstable ones. Nevertheless, the metastable states appearing in the fundamental diagram of the SOV model fend off the disturbance of randomness with a trick, i.e., the special choice of the OV function and the configuration. Since that choice allows vehicles to move with probability 1, the uniform flow continues to be stable while the uniform headway takes the value not less than the discontinuous point of the OV function. That simple consideration leads to the formula of the highest-flux density, i.e., the end-point of a metastable branch. However, all the uniform flows are not entirely stable, but higher-flux states of them are metastable, i.e., unstable against external perturbations as shown in Fig. 4. It is one of the most important things to evaluate the critical point of density where traffic flow becomes unstable and clustering of vehicles sets in.

In [7], they gave the fundamental diagram of the OV model with a practical OV function and discussed the stability of uniform flow. Then, they showed the region of density where uniform flows become unstable and gave the flux of jammed vehicles formulated analytically in the fundamental diagram. In contrast with the original OV model, the SOV model incorporates a hard-core exclusion rule, and is thus collision-free under any configuration of vehicles. Moreover, as the intention (or average velocity) is suppressed since density is high, the vehicle's motion is controlled by randomness as well as the hard-core exclusion rule. These aspects give the SOV model a fundamental diagram which is obvious different from that of the OV model.

We point out some apparent differences from the OV model attributed to the effect of hard-core exclusion rule and randomness. In the fundamental diagram of the SOV model, there is a metastable branch with positive slope (equal to the maximum velocity 1), and the jam line vanishes at a density less than 1. The simulated results reveal that the fundamental diagram of the SOV model with a step OV function consists of two line segments with which it has exactly the shape of inversed-lambda. From the diagrams, we conclude that the vehicles move approximately with either headway of free-flow or that of jammed vehicles, and our issue is thereby reduced to estimation of two specific headways. It can be done entirely by probabilistic calculations, and consequently the whole fundamental diagram (obviously including the critical point) is successfully formulated as a function of the sensitivity parameter. These analytical results are attributed to the simplicity of the SOV model and the choice of OV function.

Further studies on the SOV model under open boundary condition and on the multi-velocity version of SOV model will be given in subsequent publications [24].

## Acknowledgments

The authors appreciate Nimmo J J C for critical reading and helpful comments.

This work is supported in part by Grant-in-Aid for Scientific Research from the Japan Society for the Promotion of Science (No. 15760047).

## References

- [1] Helbing D 2001 *Rev. Mod. Phys.* **73** 1067
- [2] Chowdhury D, Santen L and Schadschneider A 2000 *Phys. Rep.* **329** 199
- [3] Nagatani T 2002 *Rep. Prog. Phys.* **65** 1331
- [4] Matsukidaira J and Nishinari K 2003 *Phys. Rev. Lett.* **90** 088701
- [5] Tokihiro T, Takahashi D, Matsukidaira J and Satsuma J 1996 *Phys. Rev. Lett.* **76** 3247
- [6] Bando M, Hasebe K, Nakayama A, Shibata A and Sugiyama Y 1995 *Phys. Rev. E* **51** 1035
- [7] Bando M, Hasebe K, Nakanishi K, Nakayama A, Shibata A and Sugiyama Y 1995 *J. Phys. I France* **5** 1389
- [8] Nagel K and Schreckenberg M 1992 *J. Phys. I France* **2** 2221
- [9] Kerner B S 2004 *The Physics of Traffic* (Berlin, New York: Springer-Verlag)
- [10] Nishinari K, Fukui M and Schadschneider A 2004 *J. Phys. A* **37** 3101
- [11] Takayasu M and Takayasu H 1993 *Fractals* **1** 860
- [12] Schadschneider A and Schreckenberg M 1997 *Ann. Physik* **6** 541
- [13] Nishinari K 2001 *J. Phys. A* **34** 10727
- [14] Newell G F 1961 *Oper. Res.* **9** 209
- [15] Kanai M, Nishinari K and Tokihiro T 2005 *Phys. Rev. E* **72** 035102(R)
- [16] Rajewsky N, Santen L, Schadschneider A and Schreckenberg M 1998 *J. Stat. Phys.* **92** 151
- [17] Schütz G M 2003 *J. Phys. A* 2003 **36** R339
- [18] Spitzer F 1970 *Adv. Math.* **5** 246
- [19] Evans M R and Hanney T 2005 *J. Phys. A* **38** R195
- [20] Klauck K and Schadschneider A 1999 *Physica A* **271** 102
- [21] Appert C and Santen L 2001 *Phys. Rev. Lett.* **86** 2498
- [22] Sugiyama Y and Yamada H 1997 *Phys. Rev. E* **55** 7749
- [23] Nakanishi K, Itoh K and Igarashi Y 1997 *Phys. Rev. E* **55** 6519
- [24] Kanai M, Nishinari K and Tokihiro T (to be published)
- [25] Schreckenberg M, Schadschneider A, Nagel K and Ito N 1995 *Phys. Rev. E* **51** 2939
- [26] O'Loan O J, Evans M R and Cates M E 1998 *Phys. Rev. E* **58** 1404